



OPEN

Derivation of mathematical closed form expressions for certain irregular topological indices of 2D nanotubes

Asad Ullah^{1,6}, Shahid Zaman^{2,6}, Arshad Hussain³, Asma Jabeen⁴ & Melaku Berhe Belay⁵

A numeric quantity that characterizes the whole structure of a network is called a topological index. In the studies of QSAR and QSPR, the topological indices are utilized to predict the physical features related to the bioactivities and chemical reactivity in certain networks. Materials for 2D nanotubes have extraordinary chemical, mechanical, and physical capabilities. They are extremely thin nanomaterials with excellent chemical functionality and anisotropy. Since, 2D materials have the largest surface area and are the thinnest of all known materials, they are ideal for all applications that call for intense surface interactions on a small scale. In this paper, we derived closed formulae for some important neighborhood based irregular topological indices of the 2D nanotubes. Based on the obtained numerical values, a comparative analysis of these computed indices is also performed.

Carbon nanotubes (CNTs) are actually cylindrical molecules that comprise of rolled-up sheets of single-layer carbon atoms (graphene). They can be single-walled having a less than 1 nm (nm) diameter or multi-walled, comprising of numerous concentrically interlinked nanotubes, with around more than 100 nm diameters. Sumio Iijima discovered the multi-walled carbon nanotubes in 1991¹. CNTs are bonded with sp^2 bonds chemically, an extremely strong form of molecular interaction. These nanotubes inherit electrical properties from graphene, which are determined by the rolling-up direction of the graphene layers. Apart from these, CNTs also have distinctive mechanical and thermal properties like light-weight, high tensile strength, low density, better thermal conductivity, high aspect ratio and high chemical stability. All these properties make them intriguing for new materials development, especially CNTs are best candidates for hydrogen storage cells, cathode ray tubes (CRTs), electronic devices, electron field emitters and transistors. Keeping in view their strong applicability and importance, it is very important to model and characterize these CNTs for a better understanding of their structural topology for enhancement of their physical properties.

The study of chemicals using a mathematical method is called mathematical chemistry. Chemical graph theory is a branch of chemistry that uses graph theory concepts to convert chemical events into mathematical models. The chemical graph is a simple connected graph in which atoms and chemical bonds are taken as vertices and edges respectively. A connected graph of order $n = |V(G)|$ and size $m = |E(G)|$ can be created with the help of G and edge set E . The focus of research in the area of nanotechnology is on atoms and Molecules. The Cartesian product of a path graph of m and n is called a 2D lattice.

Graph theory has emerged as a powerful tool for analyzing the structural properties of complex systems represented by graphs. Topological indices, which are numerical quantities derived from graph theory^{2–8}, have gained significant attention due to their ability to concisely capture important graph properties. Degree-based topological indices specifically utilize the degrees of vertices in a graph to quantify its structural characteristics⁹.

Degree based indices, such as the Randić index, the atom-bond connectivity index, and the Harary index, capture the connectivity and branching patterns in a graph by considering the distances between pairs of vertices in relation to their degrees^{10–14}. These indices have found wide applications in drug design, chemical graph theory, and network analysis^{15–18}.

¹Department of Mathematical Sciences, Karakoram International University Gilgit, Gilgit 15100, Pakistan. ²Department of Mathematics, University of Sialkot, Sialkot 51310, Pakistan. ³Karakoram International University Gilgit, Hunza Campus, Hunza, Pakistan. ⁴Department of Mathematics, University of Management and Technology, Sialkot Campus, Sialkot, Pakistan. ⁵Nanotechnology Center of Excellence, Addis Ababa Science and Technology University, P.O.Box 16417, Addis Ababa, Ethiopia. ⁶These authors contributed equally: Asad Ullah and Shahid Zaman. ✉email: dr.asadullah@kiu.edu.pk; melaku.berhe@aastu.edu.et

The Zagreb indices, including the first and second Zagreb indices, measure the sum of the vertex degrees and the product of vertex degrees, respectively^{19–21}. These degree-based indices have been successfully applied in chemistry, network analysis, and mathematical chemistry. Variants of Zagreb indices, such as the geometric-arithmetic indices and the atom-bond connectivity indices, have been developed to enhance their discriminatory power^{22–24}.

Randic-type indices, such as the augmented Zagreb index, the Randic connectivity index, and the atom-bond connectivity indices are derived from degree sequences and capture information regarding vertex degrees²⁵. These indices have found applications in chemical graph theory, network analysis, and bioinformatics^{26,27}.

Degree-based topological indices have found numerous applications across different disciplines, including chemistry, biology, materials science, and social network analysis. They have been utilized for drug design, chemical property prediction, molecular structure–property relationships, protein classification, community detection, and modeling complex networks^{28–30}.

Recent research has focused on developing new degree-based topological indices with enhanced discriminative capabilities and exploring their applications in emerging areas, such as social networks, biological networks, and complex systems. Efforts have also been made to combine degree-based indices with other topological indices to capture more comprehensive structural information. Future directions involve investigating the theoretical properties of degree-based indices, developing efficient algorithms for their computation, and exploring their applications in further real-world problems^{31–33}.

The application of Quantity Structure Activity Relationship (QSAR), which links biological structure and activity with certain constraints and properties of molecules as a result, is extensive in biology as well as in the pharmaceutical and medical fields^{34,35}. Carbon nanotubes have an intriguing role because of its special application in chemical sciences. The chemical graph theory has found significant role in thousands of topological indicators. The irregularity topological indices are listed in Table 1.

Motivated by the above formulas, we have introduced some new neighborhood version of irregular topological indices in Table 2.

Numerous efforts have been made to investigate the topological indices for various nanotubes and nanosheets in the literature. The topological invariants of Pent-Heptagonal nanosheets and $TURC_4C_8(S)$ are studied respectively in^{44,45}. The topological indices of V-phenylenic type nanotori and nanotubes have been discussed in⁴⁶, and armchair polyhex type nanotube in⁴⁷. For detailed insights into the investigations on topological modeling and analysis of micro and nanostructures, one might consult refs^{27,30,32,48–62}. Despite all these investigations, the Nano structural topology has not yet been unveiled completely. In this study, we derived closed formulae for some neighborhood version of irregular topological indices of the nanotubes $HAC_5C_7[p, q]$ and $HAC_5C_6C_7[p, q]$, and performed a comparative analysis based on the numerical results.

The $HAC_5C_7[p, q]$ nanotubes ($p, q > 1$)

A trivalent adornment has remained complete by joining C_5 and C_7 and recognized as C_5C_7 net. It has been utilized to conceal both a tube and a torus. As a C_5C_7 net, the $HAC_5C_7[p, q]$ nanotube can be studied. In 2007, Iranmanesh and Khormali calculated the vertex–Szeged index of HAC_5C_7 nanotube. The two dimensional lattice of HAC_5C_7 has been explained consistently. In the entire lattice, the number of heptagons and period are represented by p and q in row. There are $8pq + p$ vertices and $12pq - p$ edges, respectively. The three rows of HAC_5C_7 is said to be m^{th} period (Fig. 1). Consider the graph of HAC_5C_7 is represented by G . The cardinality of vertex set is $8pq + p$ and edge set is $12pq - p$ for the graph G . The vertex set is divided into three categories based on their degrees. The order of vertex V_1 is $8pq$. Similarly, $|V_2| = 2p + 2$, $|V_3| = 8pq - p - 2$. In the whole study, we denote

| Introduced by | Notation | Formula |
|--|------------|--|
| In ³⁶ , Albertson defined the Albertson index (AL) | $AL(G)$ | $\sum_{uv \in E} d_u - d_v $ |
| Vukicevic and Gasparov defined the IRL index in ³⁷ | $IRL(G)$ | $\sum_{uv \in E} nd_u - nd_v $ |
| Abdo et al. defined the total irregularity index (IRRT) in ³⁸ | $IRRT(G)$ | $\frac{1}{2} \sum_{uv \in E} d_u - d_v $ |
| Gutman introduced the IRF(G) irregularity index ³⁹ | $IRF(G)$ | $\sum_{uv \in E} (d_u - d_v)^2$ |
| The Randić index (Li and Gutman) ⁴⁰ | $IRA(G)$ | $\sum_{uv \in E} \left(d_u^{-\frac{1}{2}} - d_v^{-\frac{1}{2}} \right)^2$ |
| Reti et al. ⁴¹ | $IRDIF(G)$ | $\sum_{uv \in E} \left \frac{d_u}{d_v} - \frac{d_v}{d_u} \right $ |
| | $IRLF(G)$ | $\sum_{uv \in E} \frac{ d_u - d_v }{\sqrt{d_u d_v}}$ |
| | $LA(G)$ | $2 \sum_{uv \in E} \frac{ d_u - d_v }{(d_u + d_v)}$ |
| | $IRDI(G)$ | $\sum_{uv \in E} \ln\{1 + d_u - d_v \}$ |
| Chu and M. Abid have defined the IRGA(G) in ⁴² | $IRGA(G)$ | $\sum_{uv \in E} \ln \frac{d_u + d_v}{2\sqrt{d_u d_v}}$ |
| The bond-additive index is described in ⁴³ | $IRB(G)$ | $\sum_{uv \in E} \left(d_u^{\frac{1}{2}} - d_v^{\frac{1}{2}} \right)^2$ |

Table 1. List of the irregular topological indices.

| Notation | Formula |
|----------------|--|
| $N_{AL}(G)$ | $\sum_{uv \in E} \delta_u - \delta_v $ |
| $N_{IRL}(G)$ | $\sum_{uv \in E} \ln \delta_u - \ln \delta_v $ |
| $N_{IRRL}(G)$ | $\frac{1}{2} \sum_{uv \in E} \delta_u - \delta_v $ |
| $N_{IRF}(G)$ | $\sum_{uv \in E} (\delta_u - \delta_v)^2$ |
| $N_{IRA}(G)$ | $\sum_{uv \in E} \left(\delta_u^{\frac{-1}{2}} - \delta_v^{\frac{-1}{2}} \right)^2$ |
| $N_{IRDIF}(G)$ | $\sum_{uv \in E} \left \frac{\delta_u}{\delta_v} - \frac{\delta_v}{\delta_u} \right $ |
| $N_{IRLF}(G)$ | $\sum_{uv \in E} \frac{ \delta_u - \delta_v }{\sqrt{\delta_u \delta_v}}$ |
| $N_{LA}(G)$ | $2 \sum_{uv \in E} \frac{ \delta_u - \delta_v }{(\delta_u + \delta_v)}$ |
| $N_{IRDI}(G)$ | $\sum_{uv \in E} \ln\{1 + \delta_u - \delta_v \}$ |
| $N_{IRGA}(G)$ | $\sum_{uv \in E} \ln \frac{\delta_u + \delta_v}{2\sqrt{\delta_u \delta_v}}$ |
| $N_{IRB}(G)$ | $\sum_{uv \in E} \left(\delta_u^{\frac{1}{2}} - \delta_v^{\frac{1}{2}} \right)^2$ |

Table 2. List of the neighborhood version of irregular topological indices.

the adjacent vertices by p and q, i.e. $pq \in E_G$. The edge set is divided into the subsequent sections according to their sum of neighborhood degree, called the frequency, which is shown in Table 3.

Theorem 1 Assume that $G \in HAC_5C_7[p, q]$ then, $N_{AL}(G) = 10p$

Proof By definition of $N_{AL}(G)$ and from the neighborhood edge partitions in Table 3, one has

$$\begin{aligned}
 N_{AL}(G) &= \sum_{pq \in E} |\delta_p - \delta_q| \\
 &= (12pq - 9p)|9 - 9| + (2p)|9 - 8| + p|9 - 7| + p|8 - 8| + (2p)|8 - 6| + (2p)|7 - 6| \\
 &= 2p(1) + p(2) + 2p(2) + 2p(1) \\
 &= 2p + 2p + 4p + 2p \\
 N_{AL}(G) &= 10p
 \end{aligned}$$

Theorem 2 Assume that $G \in HAC_5C_7[p, q]$ then, $N_{IRL}(G) = 1.3705867p$

Proof Similar to the proof of theorem 1, one has

$$\begin{aligned}
 N_{IRL}(G) &= \sum_{pq \in E} |\ln \delta_p - \ln \delta_q| \\
 &= (12pq - 9p)|\ln 9 - \ln 9| + 2p|\ln 9 - \ln 8| + p|\ln 9 - \ln 7| + p|\ln 8 - \ln 8| + 2p|\ln 8 - \ln 6| + 2p|\ln 7 - \ln 6| \\
 &= 2p(2.197224 - 2.079441) + p(2.19724 - 1.94591) + 2p(2.07944 - 1.79175) + 2p(1.945910 - 1.79175)
 \end{aligned}$$

| (δ_p, δ_q) | Frequency |
|------------------------|-------------|
| (9, 9) | $12pq - 9p$ |
| (9, 8) | $2p$ |
| (9, 7) | p |
| (8, 8) | p |
| (8, 6) | $2p$ |
| (7, 6) | $2p$ |

Table 3. The neighborhood edge partitions of $HAC_5C_7[p, q]$.

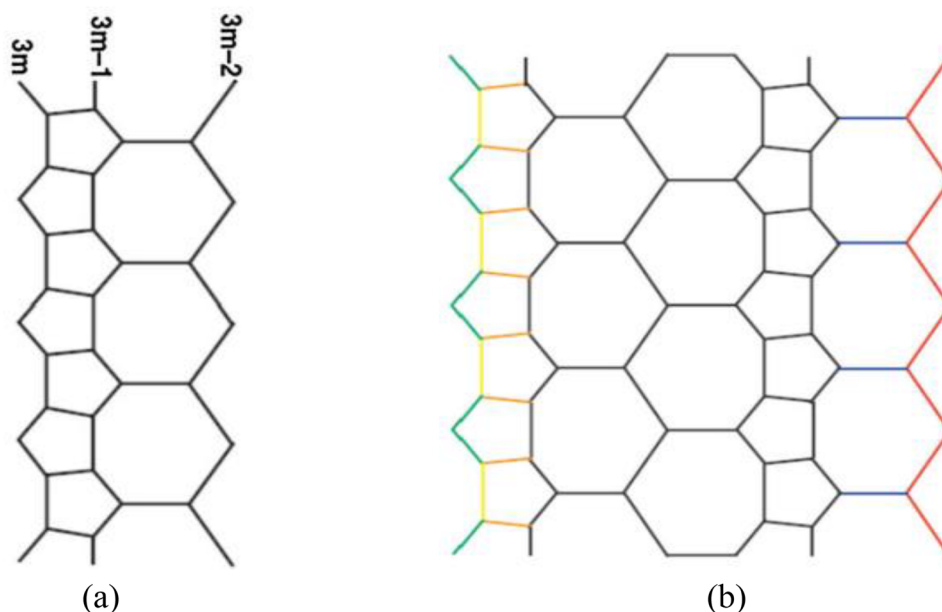


Figure 1. (a) The HAC_5C_7 nanotube $-m$ th period. (b) The HAC_5C_7 nanotube with $p=4, q=2$.

$$= 2p(0.1177835) + p(0.25133) + 2p(0.28769) + 2p(0.15416)$$

$$= 0.235567p + 0.57538p + 0.30832p + 0.25133p$$

$$N_{IRL}(G) = 1.3705867p$$

Theorem 3 Assume that $G \in HAC_5C_7[p, q]$ then, $N_{IRRT}(G) = 5p$

Proof Based on Table 3 and the definition of N_{IRRT} we have

$$N_{IRRT}(G) = \frac{1}{2} \sum_{pq \in E} |\delta_p - \delta_q|$$

$$= (12pq - 9p) \frac{1}{2} |9 - 9| + 2p \frac{1}{2} |9 - 8| + p \frac{1}{2} |9 - 7| + p \frac{1}{2} |8 - 8| + 2p \frac{1}{2} |8 - 6| + 2p \frac{1}{2} |7 - 6|$$

$$= p + p + 2p + p$$

$$N_{IRRT}(G) = 5p$$

Theorem 4 Assume that $G \in HAC_5C_7[p, q]$ then, $N_{IRF}(G) = 16p$

Proof Together Table 3 with the definition $N_{IRF}(G) = \sum_{pq \in E} (\delta_p - \delta_q)^2$, one has

$$= (12pq - 9p)(9 - 9)^2 + 2p(9 - 8)^2 + p(9 - 7)^2 + p(8 - 8)^2 + 2p(8 - 6)^2 + 2p(7 - 6)^2$$

$$= 2p + 4p + 2p(4) + 2p$$

$$= 2p + 4p + 8p + 2p$$

$$N_{IRF}(G) = 16p$$

Theorem 5 Assume that $G \in HAC_5C_7[p, q]$ then, $N_{IRA}(G) = 0.0106268538p$

Proof By definition $N_{IRA}(G) = \sum_{pq \in E} \left(\delta_p^{-\frac{1}{2}} - \delta_q^{-\frac{1}{2}} \right)^2$

$$\begin{aligned}
 &= (12pq - 9p) \left(9^{\frac{-1}{2}} - 9^{\frac{-1}{2}}\right)^2 + 2p \left(9^{\frac{-1}{2}} - 8^{\frac{-1}{2}}\right)^2 + p \left(9^{\frac{-1}{2}} - 7^{\frac{-1}{2}}\right)^2 \\
 &\quad + p \left(8^{\frac{-1}{2}} - 8^{\frac{-1}{2}}\right)^2 + 2p \left(8^{\frac{-1}{2}} - 6^{\frac{-1}{2}}\right)^2 + 2p \left(7^{\frac{-1}{2}} - 6^{\frac{-1}{2}}\right)^2 \\
 &= 2p(0.333333 - 0.353553)^2 + p(0.333333 - 0.37796)^2 + 2p(0.353553 - 0.408248)^2 + 2p(0.377964 - 0.408248)^2 \\
 &= 0.0008176968p + 0.001991836p + 0.00598308p + 0.001834241p \\
 &\text{IRA}(G) = 0.0106268538p
 \end{aligned}$$

Theorem 6 Assume that $G \in \text{HAC}_5\text{C}_7[p, q]$ then, $N_{\text{IRDIF}}(G) = 2.765846p$

Proof By definition $N_{\text{IRDIF}}(G) = \sum_{pq \in E} \left| \frac{\delta_p}{\delta_q} - \frac{\delta_q}{\delta_p} \right|$

$$\begin{aligned}
 &= (12pq - 9p) \left| \frac{9}{9} - \frac{9}{9} \right| + 2p \left| \frac{9}{8} - \frac{8}{9} \right| + p \left| \frac{9}{7} - \frac{7}{9} \right| + p \left| \frac{8}{8} - \frac{8}{8} \right| + 2p \left| \frac{8}{6} - \frac{6}{8} \right| + 2p \left| \frac{7}{6} - \frac{6}{7} \right| \\
 &= 2p(1.125 - 0.88889) + p(1.28571 - 0.77778) + 2p(1.33333 - 0.75) + 2p(1.166667 - 0.857142) \\
 &= 0.47222p + 0.50791p + 1.1666667p + 0.619056p \\
 &\text{NIRDIF}(G) = 2.765846p
 \end{aligned}$$

Theorem 7 Assume that $G \in \text{HAC}_5\text{C}_7[p, q]$ then, $N_{\text{IRLF}}(G) = 1.37363426p$

Proof By definition $N_{\text{IRLF}}(G) = \sum_{uv \in E} \frac{|\delta_p - \delta_q|}{\sqrt{\delta_p \delta_q}}$

$$\begin{aligned}
 &= (12pq - 9p) \frac{|9 - 9|}{\sqrt{9 \times 9}} + (2p) \frac{|9 - 8|}{\sqrt{9 \times 8}} + p \frac{|9 - 7|}{\sqrt{9 \times 7}} + p \frac{|8 - 8|}{\sqrt{8 \times 8}} + 2p \frac{|8 - 6|}{\sqrt{8 \times 6}} + 2p \frac{|7 - 6|}{\sqrt{7 \times 6}} \\
 &= 2p \frac{1}{\sqrt{72}} + p \frac{2}{\sqrt{63}} + 2p \frac{2}{\sqrt{48}} + 2p \frac{1}{\sqrt{42}} \\
 &= p(0.23570226) + (0.251976) + p(0.57735) + p(0.308606) \\
 &\text{NIRLF}(G) = 1.37363426p
 \end{aligned}$$

Theorem 8 Assume that $G \in \text{HAC}_5\text{C}_7[p, q]$ then, $N_{\text{LA}}(G) = 1.36441441p$

Proof By definition $N_{\text{LA}}(G) = \sum_{pq \in E} \frac{|\delta_p - \delta_q|}{(\delta_p + \delta_q)}$

$$\begin{aligned}
 &= (12pq - 9p) 2 \frac{|9 - 9|}{(9 + 9)} + (2p) 2 \frac{|9 - 8|}{(9 + 8)} + (p) 2 \frac{|9 - 7|}{(9 + 7)} + (p) 2 \frac{|8 - 8|}{(8 + 8)} + 2p(2) \frac{|8 - 6|}{(8 + 6)} + 2p(2) \frac{|7 - 6|}{(7 + 6)} \\
 &= 4p \frac{1}{17} + 2p \frac{2}{16} + 4p \frac{2}{14} + 4p \frac{1}{13} \\
 &= 0.23529411p + 0.25p + 0.571428p + 0.30769230p \\
 &\text{NLA}(G) = 1.36441441p
 \end{aligned}$$

Theorem 9 Assume that $G \in \text{HAC}_5\text{C}_7[p, q]$ then, $N_{\text{IRDI}}(G) = 6.068425221p$

Proof By definition $N_{\text{IRDI}}(G) = \sum_{pq \in E} \ln(1 + |\delta_p - \delta_q|)$

$$\begin{aligned}
 &= (12pq - 9p) \ln(1 + |9 - 9|) + 2p \ln(1 + |9 - 8|) + p \ln(1 + |9 - 7|) + p \ln(1 + |8 - 8|) + 2p \ln(1 + |8 - 6|) + 2p \ln(1 + |7 - 6|) \\
 &= (12pq - 9p) \ln 1 + 2p \ln 2 + p \ln 3 + p \ln 1 + 2p \ln 3 + 2p \ln 2 \\
 &= 1.38629436p + 1.098612p + 2.19972245p + 1.38629436p
 \end{aligned}$$

$$N_{IRDI}(G) = 6.068425221p$$

Theorem 10 Assume that $G \in HAC_5C_7[p, q]$ then, $N_{IRGA}(G) = 1.26918503p$

Proof By definition $N_{IRGA}(G) = \sum_{uv \in E} \frac{\ln|\delta_p + \delta_q|}{2\sqrt{\delta_p \delta_q}}$

$$= (12pq - 9p) \ln \frac{|9 + 9|}{2\sqrt{9 \times 9}} + 2p \ln \frac{|9 + 8|}{2\sqrt{9 \times 8}} + p \ln \frac{|9 + 7|}{2\sqrt{9 \times 7}} + p \ln \frac{|8 + 8|}{2\sqrt{8 \times 8}} + 2p \ln \frac{|8 + 6|}{2\sqrt{8 \times 6}} + 2p \ln \frac{|7 + 6|}{2\sqrt{7 \times 6}}$$

$$= 2p(0.066766) + 2p(0.696112778) + 2p(0.001733104307) + p(0.0070252649)$$

$$= 0.0034662086p + 0.0070252649p - 0.133532p + 1.392225556p$$

$$N_{IRGA}(G) = 1.26918503p$$

Theorem 11 Assume that $G \in HAC_5C_7[p, q]$ then, $N_{IRB}(G) = 0.5486855p$

Proof By definition $N_{IRB}(G) = \sum_{pq \in E} \left(\delta_p^{\frac{1}{2}} - \delta_q^{\frac{1}{2}} \right)^2$

$$= (12pq - 9p) \left(9^{\frac{1}{2}} - 9^{\frac{1}{2}} \right)^2 + 2p \left(9^{\frac{1}{2}} - 8^{\frac{1}{2}} \right)^2 + p \left(9^{\frac{1}{2}} - 7^{\frac{1}{2}} \right)^2 + p \left(8^{\frac{1}{2}} - 8^{\frac{1}{2}} \right)^2 + 2p \left(8^{\frac{1}{2}} - 6^{\frac{1}{2}} \right)^2 + 2p \left(7^{\frac{1}{2}} - 6^{\frac{1}{2}} \right)^2$$

$$= 0.058874p + 0.125492p + 0.287282p + 0.0770375p$$

$$N_{IRB}(G) = 0.5486855p$$

The $HAC_5C_6C_7[p, q]$ nanotubes ($p, q > 1$)

Let G be the graph of $HAC_5C_6C_7[p, q]$ nanotube. Then,

Theorem 12 Assume that $G \in HAC_5C_6C_7[p, q]$ be a graph as shown in Fig. 2. Then, $N_{AL}(G) = 18p$

Proof By definition of $N_{AL}(G)$ and Table 4 one has:

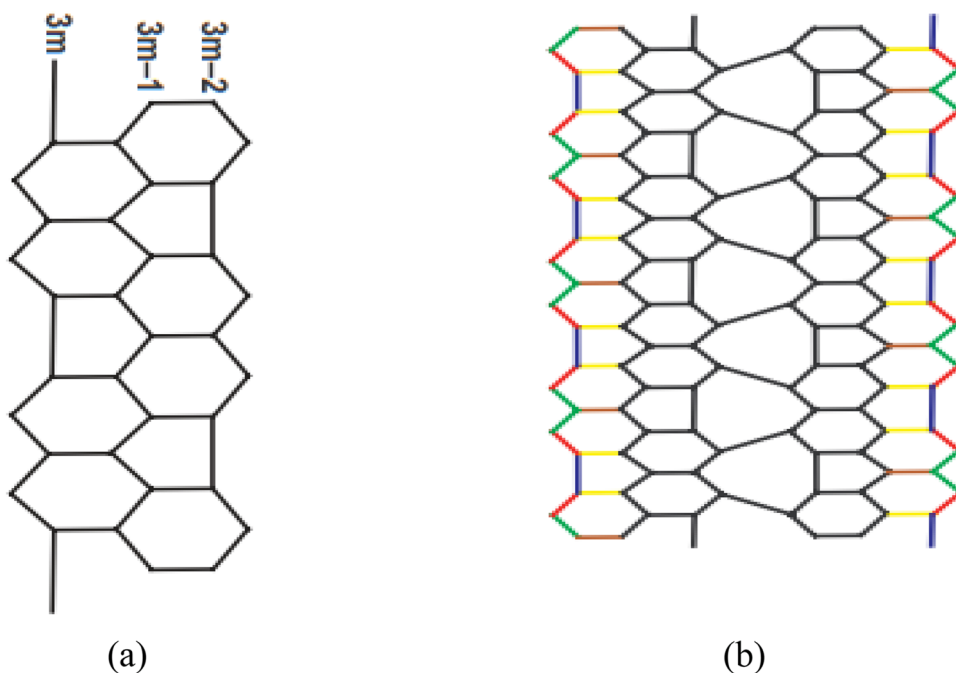


Figure 2. (a) The $HAC_5C_6C_7$ nanotube m th period, (b) The $HAC_5C_6C_7$ nanotube with $p=4$ and $q=2$.

| (δ_p, δ_q) | Frequency |
|------------------------|-------------|
| (9, 9) | $12pq - 9p$ |
| (9, 8) | $4p$ |
| (8, 8) | $2p$ |
| (8, 7) | $2p$ |
| (8, 6) | $4p$ |
| (7, 6) | $4p$ |

Table 4. The neighborhood edge partitions of $HAC_5C_6C_7$ nanotube.

$$\begin{aligned}
 N_{AL}(G) &= \sum_{pq \in E} |\delta_p - \delta_q| \\
 &= (12pq - 9p)|9 - 9| + 4p|9 - 8| + 2p|8 - 8| + 2p|8 - 7| + 4p|8 - 6| + 4p|7 - 6| \\
 &= 4p + 2p + 8p + 4p \\
 N_{AL}(G) &= 18p
 \end{aligned}$$

Theorem 13 Assume that $G \in HAC_5C_6C_7[p, q]$ be a graph as shown in Fig. 2. Then, $N_{IRL}(G) = 9p$

Proof By definition $N_{IRL}(G) = \sum_{pq \in E} |\ln \delta_p - \ln \delta_q|$

$$\begin{aligned}
 &= (12pq - 9p)|\ln 9 - \ln 9| + 4p|\ln 9 - \ln 8| + 2p|\ln 8 - \ln 8| + 2p|\ln 8 - \ln 7| + 4p|\ln 8 - \ln 6| + 4p|\ln 7 - \ln 6| \\
 &= 4p(2.197224577734 - 2.07944154168) + 2p(2.0794415 - 1.94591014906) + 4p(1.94591014906 - 1.79175946) \\
 &= 0.47113214264p + 0.26706270188p + 1.15072832672p + 0.61660275624p \\
 N_{IRL}(G) &= 2.505525927p
 \end{aligned}$$

Theorem 14 Assume that $G \in HAC_5C_6C_7[p, q]$ be a graph as shown in Fig. 2. Then, $N_{IRRT}(G) = 9p$

Proof By definition $N_{IRRT}(G) = \frac{1}{2} \sum_{pq \in E} |\delta_p - \delta_q|$

$$\begin{aligned}
 &= 4p \frac{1}{2} |9 - 8| + 2p \frac{1}{2} |8 - 8| + 2p \frac{1}{2} |8 - 7| + 4p \frac{1}{2} |8 - 6| + 4p \frac{1}{2} |7 - 6| \\
 &= 2p + p + 4p + 2p \\
 N_{IRRT}(G) &= 9p
 \end{aligned}$$

Theorem 15 Assume that $G \in HAC_5C_6C_7[p, q]$ be a graph as shown in Fig. 2. Then, $N_{IRF}(G) = 26p$

Proof By definition $N_{IRF}(G) = \sum_{pq \in E} (\delta_p - \delta_q)^2$

$$\begin{aligned}
 &= 4p(9 - 8)^2 + 2p(8 - 8)^2 + 2p(8 - 7)^2 + 4p(8 - 6)^2 + 4p(7 - 6)^2 \\
 &= 4p + 2p + 16p + 4p \\
 N_{IRF}(G) &= 26p
 \end{aligned}$$

Theorem 16 Assume that $G \in HAC_5C_6C_7[p, q]$ be a graph as shown in Fig. 2. Then, $N_{IRA}(G) = 0.0184628432p$

Proof By definition $N_{IRA}(G) = \sum_{pq \in E} \left(\delta_p^{-\frac{1}{2}} - \delta_q^{-\frac{1}{2}} \right)^2$

$$\begin{aligned}
 &= (12pq - 9p) \left(9^{-\frac{1}{2}} - 9^{-\frac{1}{2}} \right)^2 + 4p \left(9^{-\frac{1}{2}} - 8^{-\frac{1}{2}} \right)^2 + 2p \left(8^{-\frac{1}{2}} - 8^{-\frac{1}{2}} \right)^2 \\
 &\quad + 2p \left(8^{-\frac{1}{2}} - 7^{-\frac{1}{2}} \right)^2 + 4p \left(8^{-\frac{1}{2}} - 6^{-\frac{1}{2}} \right)^2 + 4p \left(7^{-\frac{1}{2}} - 6^{-\frac{1}{2}} \right)^2
 \end{aligned}$$

$$\begin{aligned}
 &= 4p(0.33333 - 0.353553)^2 + 2p(0.353553 - 0.37796)^2 + 4p(0.353553 - 0.408248)^2 + 4p(0.37796 - 0.408248)^2 \\
 &= 4p(0.00040896) + 2p(0.0005957016) + 4p(0.00299154) + 4p(0.00091736) \\
 &= 0.00163584p + 0.0011914032p + 0.01196616p + 0.00366944p
 \end{aligned}$$

$$N_{IRA}(G) = 0.0184628432p$$

Theorem 17 Assume that $G \in HAC_5C_6C_7[p, q]$ be a graph as shown in Fig. 2. Then, $N_{IRDIF}(G) = 5.051528p$

Proof By definition $N_{IRDIF}(G) = \sum_{pq \in E} \left| \frac{\delta_p}{\delta_q} - \frac{\delta_q}{\delta_p} \right|$

$$\begin{aligned}
 &= (12pq - 9p) \left| \frac{9}{9} - \frac{9}{9} \right| + 4p \left| \frac{9}{8} - \frac{8}{9} \right| + 2p \left| \frac{8}{8} - \frac{8}{8} \right| + 2p \left| \frac{8}{7} - \frac{7}{8} \right| + 4p \left| \frac{8}{6} - \frac{6}{8} \right| + 4p \left| \frac{7}{6} - \frac{6}{7} \right| \\
 &= 4p(1.125 - 0.888889) + 2p(1.14285 - 0.875) + 4p(1.3333 - 0.75) + 4p(1.1666667 - 0.85714) \\
 &= 0.9444p + 0.5357p + 2.33332p + 1.238108p
 \end{aligned}$$

$$N_{IRDIF}(G) = 5.051528p$$

Theorem 18 Assume that $G \in HAC_5C_6C_7[p, q]$ be a graph as shown in Fig. 2. Then, $N_{IRLF}(G) = 2.510484p$

Proof By definition $N_{IRLF}(G) = \sum_{pq \in E} \frac{|\delta_p - \delta_q|}{\sqrt{\delta_p \delta_q}}$

$$\begin{aligned}
 &= (12pq - 9p) \frac{|9 - 9|}{\sqrt{9 \times 9}} + 4p \frac{|9 - 8|}{\sqrt{9 \times 8}} + 2p \frac{|8 - 8|}{\sqrt{8 \times 8}} + 2p \frac{|8 - 7|}{\sqrt{8 \times 7}} + 4p \frac{|8 - 6|}{\sqrt{8 \times 6}} + 4p \frac{|7 - 6|}{\sqrt{7 \times 6}} \\
 &= 4p(0.117851) + 2p(0.1336) + 4p(0.28867) + 4p(0.15430) \\
 &= 0.471404p + 0.2672p + 1.15468p + 0.6172p
 \end{aligned}$$

$$N_{IRLF}(G) = 2.510484p$$

Theorem 19 Assume that $G \in HAC_5C_6C_7[p, q]$ be a graph as shown in Fig. 2. Then, $N_{LA}(G) = 2.495499845p$

Proof By definition $N_{LA}(G) = \sum_{pq \in E} \frac{|\delta_p - \delta_q|}{(\delta_p + \delta_q)}$

$$\begin{aligned}
 &= (12pq - 9p) 2 \frac{|9 - 9|}{(9 + 9)} + 4p(2) \frac{|9 - 8|}{(9 + 8)} + 2p(2) \frac{|8 - 8|}{(8 + 8)} + 2p(2) \frac{|8 - 7|}{(8 + 7)} + 4p(2) \frac{|8 - 6|}{(8 + 6)} + 4p(2) \frac{|7 - 6|}{(7 + 6)} \\
 &= 8p \frac{1}{17} + 4p \frac{1}{15} + 8p \frac{2}{14} + 8p \frac{1}{13} \\
 &= 0.47058823p + 0.266667p + 1.142857p + 0.615384p
 \end{aligned}$$

$$N_{LA}(G) = 2.495499845p$$

Theorem 20 Assume that $G \in HAC_5C_6C_7[p, q]$ be a graph as shown in Fig. 2. Then, $N_{IRDI}(G) = 8.553331516p$

Proof By definition $N_{IRDI}(G) = \sum_{pq \in E} \ln(1 + |\delta_p - \delta_q|)$

$$\begin{aligned}
 &= (12pq - 9p) \ln(1 + |9 - 9|) + 4p \ln(1 + |9 - 8|) + 2p \ln(1 + |8 - 8|) \\
 &\quad + 2p \ln(1 + |8 - 7|) + 4p \ln(1 + |8 - 6|) + 4p \ln(1 + |7 - 6|) \\
 &= 4p \ln(1 + 1) + 2p \ln(1 + 1) + 4p \ln(1 + 2) + 4p \ln(1 + 1) \\
 &= 4p \ln 2 + 2p \ln 2 + 4p \ln 3 + 4p \ln 2 \\
 &= 2.772588p + 1.386294361p + 4.3944915p4
 \end{aligned}$$

$$N_{IRDI}(G) = 8.553331516p$$

Theorem 21 Assume that $G \in \text{HAC}_5\text{C}_6\text{C}_7[p, q]$ be a graph as shown in Fig. 2. Then, $N_{\text{IRGA}}(G) = 0.06449422104p$

Proof By definition $N_{\text{IRGA}}(G) = \sum_{pq \in E} \frac{\ln|\delta_p + \delta_q|}{2\sqrt{\delta_p \delta_q}}$

$$= (12pq - 9p) \ln \frac{|9+9|}{2\sqrt{9 \times 9}} + 4p \ln \frac{|9+8|}{2\sqrt{9 \times 8}} + 2p \ln \frac{|8+8|}{2\sqrt{8 \times 8}} + 2p \ln \frac{|8+7|}{2\sqrt{8 \times 7}} + 4p \ln \frac{|8+6|}{2\sqrt{8 \times 6}} + 4p \ln \frac{|7+6|}{2\sqrt{7 \times 6}}$$

$$= 4p \ln \frac{17}{2\sqrt{72}} + 2p \ln \frac{15}{2\sqrt{50}} + 4p \ln \frac{14}{2\sqrt{48}} + 4p \ln \frac{13}{2\sqrt{42}}$$

$$= 0.0069324p + 0.00445435p + 0.041238p + 0.01186947p$$

$$N_{\text{IRGA}}(G) = 0.06449422104p$$

Theorem 22 Assume that $G \in \text{HAC}_5\text{C}_6\text{C}_7[p, q]$ be a graph as shown in Fig. 2. Then, $N_{\text{IRB}}(G) = 0.9130008p$

Proof By definition $N_{\text{IRB}}(G) = \sum_{pq \in E} \left(\delta_p^{\frac{1}{2}} - \delta_q^{\frac{1}{2}} \right)^2$

$$= (12pq - 9p) \left(9^{\frac{1}{2}} - 9^{\frac{1}{2}} \right)^2 + 4p \left(9^{\frac{1}{2}} - 8^{\frac{1}{2}} \right)^2 + 2p \left(8^{\frac{1}{2}} - 8^{\frac{1}{2}} \right)^2 + 2p \left(8^{\frac{1}{2}} - 7^{\frac{1}{2}} \right)^2 + 4p \left(8^{\frac{1}{2}} - 6^{\frac{1}{2}} \right)^2 + 4p \left(7^{\frac{1}{2}} - 6^{\frac{1}{2}} \right)^2$$

$$= 4p(3 - 2.828427)^2 + 2p(2.828427 - 2.645751)^2 + 4p(2.828427 - 2.449489)^2 + 4p(2.6457 - 2.4494)^2$$

$$= 0.117749p + 0.06674104p + 0.574376p + 0.15413476p$$

$$N_{\text{IRB}}(G) = 0.9130008p$$

Numerical discussion and conclusion. In this section, we conclude our work with some important remarks. In Section "The $\text{HAC}_5\text{C}_7[p, q]$ nanotubes ($p, q > 1$)" we constructed the structures of $\text{HAC}_5\text{C}_7[p, q]$ nanotubes for $p, q > 1$. Based on Fig. 1a, b, we obtained the neighborhood edge partitions as shown in Table 3. With the help of these partitions, we determined the neighborhood irregularity topological indices. Moreover,

| $[p, q]$ | N_{AL} | N_{IRL} | N_{IRRT} | N_{IRF} | N_{IRA} | N_{IRDIF} | N_{IRLF} | N_{LA} | N_{IRDI} | N_{IRGA} | N_{IRB} |
|----------|----------|-----------|------------|-----------|-----------|-------------|------------|----------|------------|------------|-----------|
| [1, 1] | 10 | 1.37 | 5 | 16 | 0.01 | 2.76 | 1.37 | 1.36 | 6.06 | 1.26 | 0.54 |
| [2, 2] | 20 | 2.74 | 10 | 32 | 0.02 | 5.53 | 2.75 | 2.72 | 12.13 | 2.53 | 1.09 |
| [3, 3] | 30 | 4.11 | 15 | 48 | 0.03 | 8.29 | 4.12 | 4.09 | 18.20 | 3.80 | 1.64 |
| [4, 4] | 40 | 5.48 | 20 | 64 | 0.04 | 11.06 | 5.54 | 5.45 | 24.27 | 5.07 | 2.19 |
| [5, 5] | 50 | 6.87 | 25 | 80 | 0.05 | 13.82 | 6.86 | 6.82 | 30.34 | 6.34 | 2.74 |
| [6, 6] | 60 | 8.25 | 30 | 96 | 0.06 | 16.59 | 8.24 | 8.18 | 36.41 | 7.61 | 3.2 |

Table 5. Comparison of computed indices for $\text{HAC}_5\text{C}_7[p, q]$ nanotube.

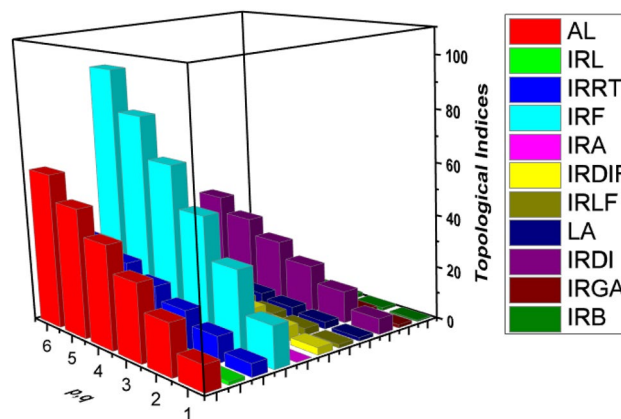


Figure 3. Comparison graph for $\text{HAC}_5\text{C}_7[p, q]$ nanotube.

| $[p, q]$ | N_{AL} | N_{IRL} | N_{IRRT} | N_{IRF} | N_{IRA} | N_{IRDIF} | N_{IRLF} | N_{LA} | N_{IRDI} | N_{IRGA} | N_{IRB} |
|----------|----------|-----------|------------|-----------|-----------|-------------|------------|----------|------------|------------|-----------|
| [1, 1] | 18 | 2.50 | 9 | 26 | 0.01 | 5.05 | 2.51 | 2.49 | 8.55 | 0.06 | 0.91 |
| [2, 2] | 36 | 65.04 | 18 | 52 | 0.03 | 10.10 | 5.020 | 4.99 | 17.10 | 0.12 | 1.82 |
| [3, 3] | 54 | 7.51 | 27 | 78 | 0.05 | 15.15 | 7.53 | 7.48 | 25.65 | 0.19 | 2.73 |
| [4, 4] | 72 | 10.02 | 36 | 104 | 0.07 | 20.20 | 10.04 | 9.98 | 34.21 | 0.25 | 3.65 |
| [5, 5] | 90 | 12.52 | 45 | 130 | 0.09 | 25.25 | 12.55 | 12.47 | 42.76 | 0.32 | 4.56 |
| [6, 6] | 108 | 15.03 | 54 | 156 | 0.12 | 30.30 | 15.06 | 14.97 | 51.31 | 0.38 | 5.47 |

Table 6. Comparison of computed indices for $HAC_5C_6C_7[p, q]$ nanotube.

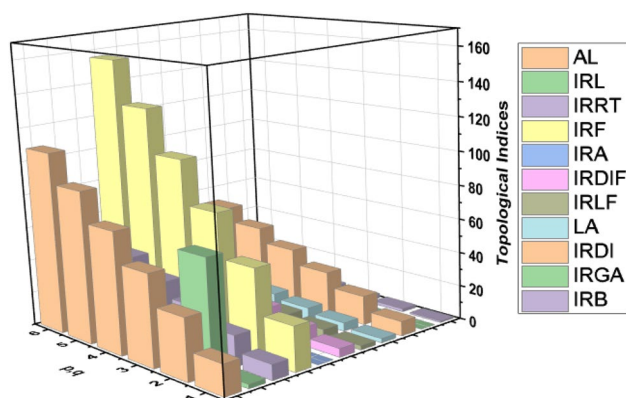


Figure 4. Comparison graph for $HAC_5C_6C_7[p, q]$ nanotube.

the numerical and graphical comparisons among all considered topological indices are given in Table 5 and Fig. 3. Which shows that there is a positive relation between p, q and these topological indices. That is to say, when we increase the values of p and q the values of topological indices also increase. Hence, from this comparison it is easy to see that the value of N_{IRF} index is higher than the values of remaining topological indices.

In Section "The $HAC_5C_6C_7[p, q]$ nanotubes ($p, q > 1$)", we constructed the structures of $HAC_5C_6C_7[p, q]$ nanotubes for $p, q > 1$. Based on Fig. 2a, b, we obtained the edge partitions as shown in Table 4. With the help of these edge partitions, we determined the neighborhood irregularity topological indices. Moreover, the numerical and graphical comparisons among all considered topological indices are given in Table 6 and Fig. 4. Which shows that there is a positive relation between p, q and these topological indices, when we increase the values of p and q , the values of topological indices also increase. Hence, from this comparison it is easy to see that the value of N_{IRF} index is higher than the values of remaining topological indices.

Data availability

All data generated or analysed during this study are included in this article.

Received: 2 April 2023; Accepted: 7 July 2023

Published online: 11 July 2023

References

- Iijima, S. Helical microtubules of graphitic carbon. *Nature* **354**, 56–58 (1991).
- Liu, J.-B. & Zhao, B.-Y. Study on environmental efficiency of Anhui province based on SBM-DEA model and fractal theory. *Fractals* <https://doi.org/10.1142/S0218348X23400728> (2023).
- Liu, J.-B., Peng, X.-B. & Zhao, J. Analyzing the spatial association of household consumption carbon emission structure based on social network. *J. Comb. Optim.* **45**, 79 (2023).
- Zaman, S., Yaqoob, H.S.A., Ullah, A. & Sheikh, M. QSPR Analysis of some novel drugs used in blood cancer treatment via degree based topological indices and regression models, *Polycyc. Aromatic Compd.* 1-17 (2023).
- Zaman, S., Salman, M., Ullah, A., Ahmad, S. & Abdelgader Abas, M. S. Three-dimensional structural modelling and characterization of sodalite material network concerning the irregularity topological indices. *J. Math.* <https://doi.org/10.1155/2023/5441426> (2023).
- Kosar, Z., Zaman, S. & Siddiqui, M. K. Structural characterization and spectral properties of hexagonal phenylene chain network. *Eur. Phys. J. Plus* **138**, 415 (2023).
- Liu, J.-B., Xie, Q. & Gu, J.-J. Statistical analyses of a class of random pentagonal chain networks with respect to several topological properties. *J. Funct. Spaces* <https://doi.org/10.1155/2023/6675966> (2023).
- Ahmad, A., Koam, A. N. & Azeem, M. Reverse-degree-based topological indices of fullerene cage networks. *Mole. Phys.* <https://doi.org/10.1080/00268976.2023.2212533> (2023).
- Randic, M. Characterization of molecular branching. *J. Am. Chem. Soc.* **97**, 6609–6615 (1975).
- Robins, G. A tutorial on methods for the modeling and analysis of social network data. *J. Math. Psychol.* **57**, 261–274 (2013).

11. Hakeem, A., Ullah, A. & Zaman, S. Computation of some important degree-based topological indices for γ -graphyne and Zigzag graphyne nanoribbon. *Mole. Phys.* <https://doi.org/10.1080/00268976.2023.2211403> (2023).
12. Zaman, S., Jalani, M., Ullah, A., Ali, M. & Shahzadi, T. On the topological descriptors and structural analysis of cerium oxide nanostructures. *Chem. Pap.* **77**, 2917–2922 (2023).
13. Gutman, I. & Trinajstić, N. Graph theory and molecular orbitals. Total π -electron energy of alternant hydrocarbons. *Chem. Phys. Lett.* **17**, 535–538 (1972).
14. Koam, A. N., Ahmad, A., Baća, M. & Semaničová-Feňovčíková, A. Modular edge irregularity strength of graphs. *AIMS Math.* **8**, 1475–1487 (2023).
15. Bonchev, D. & Trinajstić, N. Information theory, distance matrix, and molecular branching. *J. Chem. Phys.* **67**, 4517–4533 (1977).
16. Huang, Q. *et al.* Breast cancer chemical structures and their partition resolvability. *Math. Biosci. Eng.* **20**, 3838–3853 (2022).
17. Ullah, A., Bano, Z. & Zaman, S. Computational aspects of two important biochemical networks with respect to some novel molecular descriptors. *J. Biomole. Struct. Dyn.*, 1–15 (2023).
18. Zaman, S., Jalani, M., Ullah, A., Ahmad, W. & Saeedi, G. Mathematical analysis and molecular descriptors of two novel metal-organic models with chemical applications. *Sci. Rep.* **13**, 5314 (2023).
19. Siddiqui, M. K., Imran, M. & Ahmad, A. On Zagreb indices Zagreb polynomials of some nanostar dendrimers. *Appl. Math. Comput. Biol.* **280**, 132–139 (2016).
20. Yan, T., Kosar, Z., Aslam, A., Zaman, S. & Ullah, A. Spectral techniques and mathematical aspects of K 4 chain graph. *Phys. Scr.* **98**, 045222 (2023).
21. Dinar, J., Hussain, Z., Zaman, S. & Rehman, S. U. Wiener index for an intuitionistic fuzzy graph and its application in water pipeline network. *Ain Shams Eng. J.* **14**, 101826 (2023).
22. Emadi Kouchak, M., Safaei, F. & Reshadi, M. Graph entropies-graph energies indices for quantifying network structural irregularity. *J. Supercomput.* **79**, 1705–1749 (2023).
23. Zhao, X., Siddiqui, M.K., Manzoor, S., Ahmad, S., Muhammad, M.H., & Liu, J.-B. On Computation and analysis of entropy measures for metal-insulator transition super lattice, IETE J. Res., 1–12 (2023).
24. Yu, X., Zaman, S., Ullah, A., Saeedi, G. & Zhang, X. Matrix analysis of hexagonal model and its applications in global mean-first-passage time of random walks. *IEEE Access* **11**, 10045–10052 (2023).
25. Estrada, E. Characterization of 3D molecular structure. *Chem. Phys. Lett.* **319**, 713–718 (2000).
26. Mauri, A., Consonni, V. & Todeschini, R. *Molecular descriptors 2065–2093* (Springer, 2017).
27. Zaman, S. & Ullah, A. Kemeny's constant and global mean first passage time of random walks on octagonal cell network. *Math. Methods Appl. Sci.* **46**, 9177–9186 (2023).
28. Wiener, H. Structural determination of paraffin boiling points. *J. Am. Chem. Soc.* **69**, 17–20 (1947).
29. Zaman, S. & He, X. Relation between the inertia indices of a complex unit gain graph and those of its underlying graph. *Linear Multilinear Algebra* **70**, 843–877 (2022).
30. Zaman, S., Jalani, M., Ullah, A. & Saeedi, G. Structural analysis and topological characterization of Sudoku nanosheet. *J. Math.* **2022**, 1–10 (2022).
31. Zhou, B. On the energy of a graph, Kragujevac J. Sci., 5–12 (2004).
32. Zaman, S. Spectral analysis of three invariants associated to random walks on rounded networks with 2 n-pentagons. *Int. J. Comput. Math.* **99**, 465–485 (2022).
33. Zaman, S. & Ali, A. On connected graphs having the maximum connective eccentricity index, J. Appl. Math. Comput., 1–12 (2021).
34. Kuli, V. R. Some topological indices of certain nanotubes. *J. Comput. Math. Sci.* **8**, 1–7 (2017).
35. Parvathi, V. L. K. N. Computation of topological indices of HA (C5c6c7) nanotube. *Ann. Roman. Soc. Cell Biol.* **25**, 3080–3085 (2021).
36. Albertson, M. O. The irregularity of a graph. *Ars Combin.* **46**, 219–225 (1997).
37. Vukičević, D. & Graovac, A. Valence connectivity versus Randić Zagreb and modified Zagreb index: A linear algorithm to check discriminative properties of indices in acyclic molecular graphs. *Croatica Chemica Acta* **77**, 501–508 (2004).
38. Dimitrov, D., Brandt, S. & Abdo, H. The total irregularity of a graph. *Discrete Math. Theor. Comput. Sci.* <https://doi.org/10.46298/dmtcs.1263> (2014).
39. Gutman, I. Topological indices and irregularity measures. *Bull.* **8**, 469–475 (2018).
40. Li, X. & Gutman, I. *Mathematical aspects of randic-type molecular structure descriptors* (University of Kragujevac Kragujevac, Serbia, 2006).
41. Réti, T., Sharafzadeh, R., Dregelyi-Kiss, A. & Haghbin, H. Graph irregularity indices used as molecular descriptors in QSPR studies. *MATCH Commun. Math. Comput. Chem.* **79**, 509–524 (2018).
42. Chu, Y.-M., Abid, M., Qureshi, M. I., Fahad, A. & Aslam, A. Irregular topological indices of certain metal organic frameworks. *Main Group Met. Chem.* **44**, 73–81 (2020).
43. Avdullahu, A. & Filipovski, S. On certain topological indices of graphs, arXiv preprint [arXiv:2210.12981](https://arxiv.org/abs/2210.12981), DOI (2022).
44. Gao, Y. Y., Sardar, M. S., Hosamani, S. M. & Farahani, M. R. Computing sanskruti index of TURC4C8 (s) nanotube. *Int. J. Pharm. Sci. Res.* **8**, 4423–4425 (2017).
45. Deng, F., Zhang, X., Alaeiyan, M., Mehboob, A. & Farahani, M. R. Topological indices of the pent-heptagonal nanosheets VC5C7 and HC5C7. *Adv. Mater. Sci. Eng.* **2019**, 1–12 (2019).
46. Jiang, H. *et al.* Computing Sanskruti index of V-phenylenic nanotubes and nanotori. *Int. J. Pure Appl. Math.* **115**, 859–865 (2017).
47. Farahani, M. R. Computing GA5 index of armchair polyhex nanotube. *Matematiche (Catania)* **69**, 69–76 (2014).
48. Ullah, A., Qasim, M., Zaman, S. & Khan, A. Computational and comparative aspects of two carbon nanosheets with respect to some novel topological indices. *Ain Shams Eng. J.* **13**, 101672 (2022).
49. Ullah, A., Zeb, A. & Zaman, S. A new perspective on the modeling and topological characterization of H-Naphtalenic nanosheets with applications. *J. Mol. Model.* **28**, 211 (2022).
50. Wang, H., Liu, G., Ullah, A. & Luan, J. Topological correlations of three-dimensional grains. *Appl. Phys. Lett.* **101**, 041910 (2012).
51. Wenwen, L. *et al.* Topological correlations of grain faces in polycrystal with experimental verification. *EPL (Europhys. Lett.)* **104**, 56006 (2013).
52. Ullah, A. *et al.* Three-dimensional visualization and quantitative characterization of grains in polycrystalline iron. *Mater. Characteriz.* **91**, 65–75 (2014).
53. Asad, U. *et al.* Neighborhood topological effect on grain topology-size relationship in three-dimensional polycrystalline microstructures. *Chin. Sci. Bull.* **58**, 3704–3708 (2013).
54. Ullah, A., Shamsudin, Zaman, S., Hamraz, A. & Saeedi, G. Network-based modeling of the molecular topology of fuchsine acid dye with respect to some irregular molecular descriptors. *J. Chem.* **2022**, 1–8 (2022).
55. Zaman, S., Abolaban, F. A., Ahmad, A. & Asim, M. A. Maximum H-index of bipartite network with some given parameters. *AIMS Math.* **6**, 5165–5175 (2021).
56. Zaman, S. Cacti with maximal general sum-connectivity index. *J. Appl. Math. Comput.* **65**, 147–160 (2021).
57. Khabyah, A. A., Zaman, S., Koam, A. N. A., Ahmad, A. & Ullah, A. Minimum Zagreb eccentricity indices of two-mode network with applications in boiling point and Benzenoid hydrocarbons. *Mathematics* **10**, 1393 (2022).
58. Ullah, A. *et al.* Optimal approach of three-dimensional microstructure reconstructions and visualizations. *Mater. Express* **3**, 109–118 (2013).

59. Zaman, S., Koam, A. N. A., Khabyah, A. A. & Ahmad, A. The Kemeny's constant and spanning trees of hexagonal ring network. *Comput. Mater. Continua* **73**, 6347 (2022).
60. Ullah, A. *et al.* Simulations of grain growth in realistic 3D polycrystalline microstructures and the MacPherson–Srolovitz equation. *Mater. Res. Express* **4**, 066502 (2017).
61. Ullah, A., Shaheen, M., Khan, A., Khan, M. & Iqbal, K. Evaluation of topology-dependent growth rate equations of three-dimensional grains using realistic microstructure simulations. *Mater. Res. Express* **6**, 026523 (2018).
62. Ullah, A., Shamsudin, S. & Zaman, A. H. Zagreb connection topological descriptors and structural property of the triangular chain structures. *Phys. Scr.* **98**, 025009 (2023).

Author contributions

The authors A.U. and S.Z. have equally contributed to this manuscript in all stages, from conceptualization to the write-up of final draft. A.H., A.J. and M.B. Belay contributed in methodology, results and analysis.

Funding

No funding was available for this study.

Competing interests

The authors declare no competing interests.

Additional information

Correspondence and requests for materials should be addressed to A.U. or M.B.B.

Reprints and permissions information is available at www.nature.com/reprints.

Publisher's note Springer Nature remains neutral with regard to jurisdictional claims in published maps and institutional affiliations.



Open Access This article is licensed under a Creative Commons Attribution 4.0 International License, which permits use, sharing, adaptation, distribution and reproduction in any medium or format, as long as you give appropriate credit to the original author(s) and the source, provide a link to the Creative Commons licence, and indicate if changes were made. The images or other third party material in this article are included in the article's Creative Commons licence, unless indicated otherwise in a credit line to the material. If material is not included in the article's Creative Commons licence and your intended use is not permitted by statutory regulation or exceeds the permitted use, you will need to obtain permission directly from the copyright holder. To view a copy of this licence, visit <http://creativecommons.org/licenses/by/4.0/>.

© The Author(s) 2023